Orbiting Carbon Observatory-2 & 3
(OCO-2 & OCO-3)

Orbiting Carbon Observatory-3 (OCO-3)
Data Quality Statement:
Level 2 Forward and Retrospective Processing
Data Release 10 (v10 and v10r)

Version 2.0 Rev 2
September 1, 2021

National Aeronautics and
Space Administration

Jet Propulsion Laboratory
California Institute of Technology
Pasadena, California

Orbiting Carbon Observatory-3 (OCO-3)
Data Quality Statement: Level 2 Forward Processing Data Release 10 (v10)

Annmarie Eldering	Jet Propulsion Laboratory
Robert Rosenberg	Jet Propulsion Laboratory
Matthäus Kiel	Jet Propulsion Laboratory
Brendan Fisher	Jet Propulsion Laboratory
Robert Nelson	Jet Propulsion Laboratory
Lan Dang	Jet Propulsion Laboratory
Christopher O’Dell	Colorado State University
Tommy Taylor	Colorado State University
Gregory Osterman	Jet Propulsion Laboratory

Document History:

Version	Revision	Date	Description/Comments
1.0	1	April 30, 2020	Data Quality Statement for OCO-3 vEarly
2.0	1	August 1, 2021	Updated for new data release, v10
2.0	2	Sept. 2, 2021	Minor revisions and notes on v10r

The research described in this document was carried out at the Jet Propulsion Laboratory,
California Institute of Technology, under a contract with the
National Aeronautics and Space Administration.

TABLE OF CONTENTS

LIST OF FIGURES

LIST OF TABLES

No tables found.

1 Data Quality Statement

The Orbiting Carbon Observatory (OCO-3) has released the second version of the Level 2 (L2) forward processing data product, containing estimates of the column averaged carbon dioxide dry air mole fraction (X_{CO2}) and other geophysical quantities retrieved from OCO-3 observations. This version of the L2 Product is release 10 (v10) and begins with August 2019 data. The full OCO-3 L2 data set with complete reprocessing back to August 2019 will be completed and posted at the Goddard Earth Sciences Data and Information Services Center later in 2021. Updated documentation, L2 Data Users' Guide, will be made available before the completion of the reprocessing.

The L2 algorithms used are the same as those that are used for the current OCO-2 v10 L2 data release, to aid in the use of the two datasets together.

There are no known issues in the OCO-3 v10 data as of August 2021. The issues in the vEarly OCO-3 data related to errors in the L1b radiometric calibration and geolocation have been corrected for the v10 release. Users' should be aware that the geolocation of the retrospective product in some cases will be superior to the forward stream of the data.

1.1 Radiometric errors

The radiometric calibration of v10 is significantly improved. In contrast to vEarly, which contains a discontinuity at April 8, 2020, all lamp data across the entire mission has been processed with the same algorithms. The key improvement for v10 which was introduced midway through vEarly was to tie radiometric degradation to Lamp 1, which is used roughly once a week. Initially, Lamp 3 was being used with no correction for lamp aging. Additionally, v10 featured an updated stray light model which aims to account for spatial variability.

Since the focal plane arrays are operated at cryogenic temperatures, ice accumulates over time, leading to increased stray light and decreased throughput. Several decontaminations have been performed to counteract this. The largest discontinuity in the gain degradation record (Fig 1) occurs following the decon from solarday 9720, which was nearly a year after the previous one.

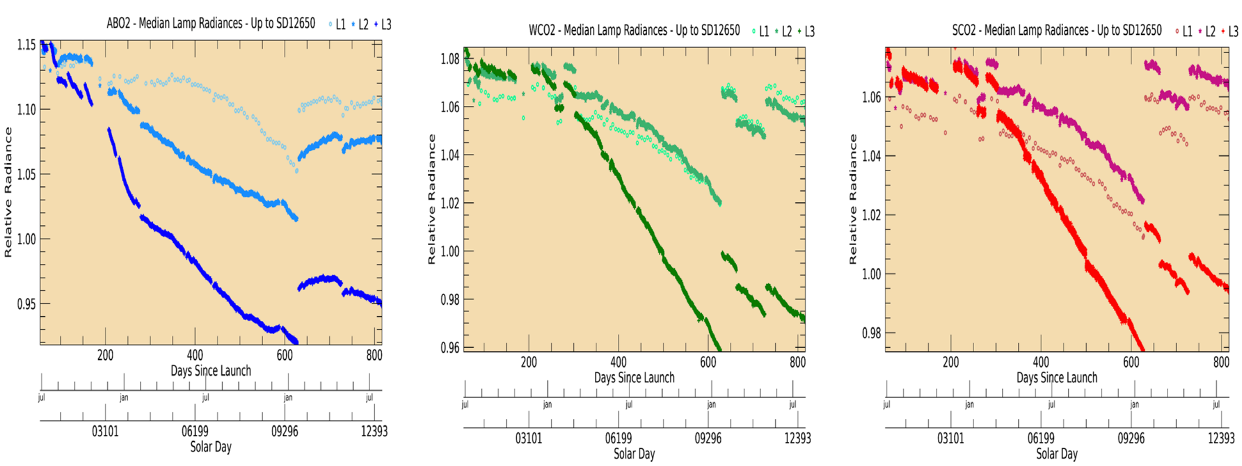

Figure 1-1: Lamp radiance trends relative to prelaunch over the course of the OCO-3 mission. The three panels are for the ABO2, WCO2, and SCO2 channels. Within each panel, different colors indicate different lamps. Lamp 3 is used roughly 12 times per day, Lamp 2 is used roughly 3 times per day, and Lamp 1 is used roughly 1 time per week.

A key indicator of calibration improvements is the reduction in time dependent and footprint dependent behavior in the L2 data. The science team examined the behavior of dP, a parameter in the retrieval that is very sensitive to ABO2 radiometric calibration. We found that this parameter is stable in v10, with some increase in value correlated with detector icing. The increase is largest from June 2020 to Jan 2021. The dP test data record (Fig 2) ends in Dec 2020, just before the major decontamination event.

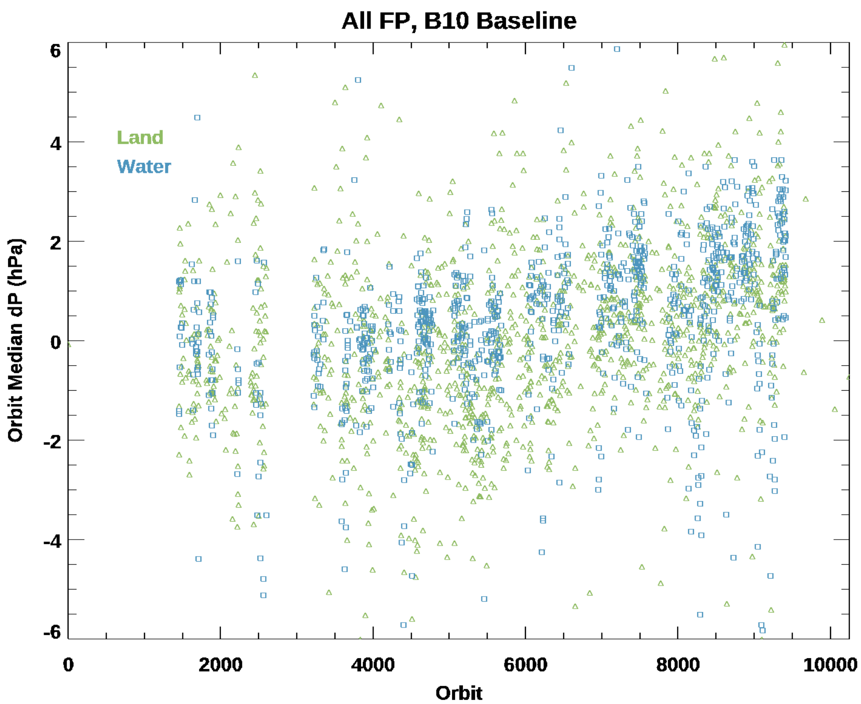

Figure 1-2: L2 dP values from OCO-3 v10 test data from Aug 2019 to Dec 2020.

There is some variation in the dP values among footprints, which is consistent with our understanding that icing impacts are spatially nonuniform, but the magnitude is substantially reduced from vEarly. This is also seen in the throughput of data in L2 which worsened later in the vEarly record, especially for high numbered footprints. This pattern is not seen in v10.

1.2 Geolocation errors

Geolocation errors have been substantantially improved for v10 in three general areas. First, calibration of the Pointing Mirror Assembly (PMA) is completed and integrated directly into the gelocation algorithm. Second, an offset between the science detectors and the PMA camera was characterized and removed. Third, the OCO-3 project has obtained a supplemental attitude source, derived from the CALET instrument which is near OCO-3 on the JEM-EF, for periods when the OCO-3 Stellar Reference Unit (SRU) is not available. The supplemental attitude data reduces geolocation errors associated with flexure between the ISS center, where the primary ISS ephemeris is reported, and the OCO-3 location on the JEM-EF. For periods when the OCO-3 SRU is available, geolocation errors are typically less than 500 m. For periods where the SRU is not available and CALET-derived attitude is available, errors are typically less than 1 km. Finaly, a small percentage of the data remains when neither of the two primary attitude sources are available, and for these periods the errors are typically less than 2 km, with a small "tail" with errors up to 3 km. The OCO-3 L2 products now contain a new field, /RetrievalGeometry/retrieval_att_data_source. A value of 1 in this field represents the "no supplemental attitude" case, with the largest errors. Other values in the range 2-9, have good geolocation, with the errors listed above. The different numbers in the 2-9 range represent various permutations of SRU and CALET, accounting for nominal operations with the possibility of small gaps.

The improvements that rely on the CALET data are only available in the retrospective processing (v10r). In the forward stream processing, we rely soley on the OCO-3 SRU and ISS BAD data, so geolocation performance may be poorer than in the retrospective data. The attitude source information that is included in the product can help the user to differentiate these cases. More details will be in the Data Users' Guide.

1.3 Validation Status

The fundamental means for tying the OCO-3 X_{CO2} to the World Meteorological Organization's CO_2 standard is by comparison with ground-based observations from the Total Carbon Column Observing Network (TCCON). A description of the process of validating OCO-2 data against TCCON is described in Wunch et al. (2017) using an earlier OCO-2 data version. The OCO-2 validation plan was first described prior to launch in an analysis using TCCON and X_{CO2} estimates retrieved using the OCO-2 retrieval algorithm on data from JAXA's GOSAT satellite (Wunch et al, 2011b). To derive quality filtering and bias correction, we follow the methods described in O'Dell et al. (2018). We compare the retrieved X_{CO2} to an independent estimate of X_{CO2}, a so-called truth proxy. For OCO-3 v10, we used three different truth proxy data sets: TCCON, a small area approximation (SAA), and a truth proxy based on results from global carbon flux inverse models ("multi-model median").

The TCCON truth proxy includes data from 19 TCCON stations. We use the GGG2014 dataset covering the time period between August 2019 and December 2020 and spanning from 55°N to 45°S in latitude. We use similar coincidence criteria as O'Dell et al., (2018) to match airmasses observed by TCCON and OCO-3. In total we count ~101K coincident soundings between OCO-3 and TCCON in nadir mode over land, ~91K coincident soundings in SAM/target mode, and 18K soundings in glint mode over water.

The SAA truth proxy (for more details see O'Dell et al.,2018) makes use of the low spatial variability of X_{CO2} over small regions (up to 100 km) and short time spans (~10 s). Here we define continuous segments of soundings that were collected along-track within ~10 s as small areas. Between August 2019 and December 2020, the SAA truth proxy consists of ~656K soundings in nadir mode over land, ~219K soundings in SAM/target mode, and ~ 869K soundings in glint mode over water.

A suite of four models sampled at OCO-3 sounding locations and times was used for the multi-model median truth proxy (for more details see O'Dell et al.,2018). The models generally differ in their prior flux assumptions, prior flux uncertainty, transport model, initial conditions, spatial resolution, and inverse method. Each model assimilates either in-situ CO_2 concentration data, GOSAT XCO_2 data, OCO-2 XCO_2 data, or a combination of the above. Between August 2019 and December 2020, the multi-model median truth proxy consists of ~1358K soundings in nadir mode over land, ~797K soundings in SAM/target mode, and ~ 1500K soundings in glint mode over water.

All three truth proxy data sets were used to derive quality filters, which utilize different parameters within the L2 data product. Further, a footprint and parametric bias correction formula has been determined that allows for adjusting the OCO-3 data consistent with biases seen relative to the truth proxy data sets. In addition, for observations over land, a global scaling factor of 0.9963 was determined to tie OCO-3 XCO_2 data to the WMO CO_2 standard scale (through direct comaprisons to TCCON). For observations over water, a global scaling factor of 0.9961 was determind (using a multi-model median and coastline bootstrap method).

A first comparison between co-located TCCON and filtered and bias corrected X_{CO2}, indicates a single sounding root mean squared error (RMSE) of 1.33 ppm for nadir observations over land, 1.31 ppm for SAM/target observations, and 0.99 ppm for glint observations over water. The v10 bias correction also reduces swath biases that were apparent in OCO-3's vEarly SAM and target mode observations.

1.4 Summary

Overall, OCO-3 v10 X_{CO2} shows very good performance for all three modes of data collection. A more detailed validation and evaluation study of OCO-3 X_{CO2} against TCCON, model data, COCCON, and cross comparisons against OCO-2 will be included in the data users guide. The OCO-2 and OCO-3 data are now both released in v10, which will support the science community in the use of the datasets together.

There is much more documentation that will help with utilizing the OCO-3 L2 data, all of which is available at the GES DISC OCO-3/OCO-2 documentation page (https://disc.gsfc.nasa.gov/information/documents?title=OCO-2%20Documents). Note that OCO-2 and OCO-3 have combined documents. For example, the L2 ATBD will describe the common algorithm as well as mission specific features and the small number of differences in the data fields.

2 References

A. Eldering et al., The OCO-3 mission: measurement objectives and expected performance based on 1 year of simulated data, Atmos. Meas. Tech., 12, 4, 2341-2370, 2019. https://doi.org/10.5194/amt-12-2341-2019

M. Kiel, et al., How bias correction goes wrong: measurement of X_{CO2} affected by erroneous surface pressure estimates, 12, 2241-2259, 2019. https://doi.org/10.5194/amt-12-2241-2019

C. O'Dell et al., Improved retrievals of carbon dioxide from Orbiting Carbon Observatory-2 with the version 8 ACOS algorithm, Atmos. Meas. Tech., 11, 6539-6576, 2018. https://doi.org/10.5194/amt-11-6539-2018

D. Wunch et al., Comparisons of the Orbiting Carbon Observatory-2 (OCO-2) X_{CO2} measurements with TCCON, Atmos. Meas. Tech., 10, 2209–2238, 2017. https://doi.org/10.5194/amt-10-2209-2017

D. Wunch et al., A method for evaluating bias in global measurements of CO_2 total columns from space, Atmos. Chem. Phys., 11, 12317–12337, 2011. https://doi.org/10.5194/acp-11-12317-2011